Space Weather

RESEARCH ARTICLE
10.1029/2022SW003412

Special Section:
Small Satellites for Space Weather Research and Forecasting Workshops

Numerical Calculations of Charging Threshold at GEO Altitudes With Two Temperature Non-Extensive Electrons

Saba Javed[1], Nazish Rubab[2,3], Sadia Zaheer[1], Stefaan Poedts[3,4], and Ghulam Jaffer[5]

[1]Department of Physics, Forman Christian College (A Chartered University), Lahore, Pakistan, [2]Department of Physics, University of Central Punjab, Lahore, Pakistan, [3]Centre for Mathematical Plasma Astrophysics, Department of Mathematics, KU Leuven, Leuven, Belgium, [4]Institute of Physics, University of Maria Curie-Skłodowska, Lublin, Poland, [5]Space System Engineering, SnT - Interdisciplinary Centre for Security, Reliability and Trust, University of Luxembourg, Esch-sur-Alzette, Luxembourg

Abstract Surface charging at geosynchronous altitude is one of the major concerns for satellites and spacecrafts. Spacecraft anomalies are often associated with extreme surface charging events, especially during substorms in which the GEO plasma is better modeled as two temperatures non-Maxwellian plasma. In such case, we employ two temperature q-non-extensive distribution function to determine the onset of spacecraft surface charging which becomes complex since many parameters control the surface charging. We developed a current balance equation which better explains the charging threshold in comparison to a Maxwellian distribution function. The effect of non-extensive parameters, temperature and density ratio on the current balance equation has been explained. The modified current balance equation predicts the critical and anti-critical temperatures for various space-grade materials both analytically and numerically. A significant change is observed in the quantities characterizing the charging current, average yield and density ratio in the presence of non-extensive two temperature electrons. The mechanism underlying different charging behaviors at or near the threshold is also indicated at various plasma parametric domains. Furthermore, the general conditions of potential jump are also obtained theoretically which predicts the sudden or smooth potential transition.

Plain Language Summary Spacecraft Charging at Geosynchronous altitudes is determined with two temperature non-extensive distribution function. A modified current balance equation and charging behaviors at the threshold are elucidated. The effect of the q-parameter is examined by selecting various space-grade materials.

Key Points:

- Spacecraft charging at GEO altitude is modeled by using two temperature non-extensive electrons
- The modified threshold condition is derived to determine the critical and anti-critical temperatures for various space-grade materials
- The present model provides a more realistic situation of the surface charging phenomenon near threshold condition

Correspondence to:
N. Rubab,
drnrubab@gmail.com

Citation:
Javed, S., Rubab, N., Zaheer, S., Poedts, S., & Jaffer, G. (2023). Numerical calculations of charging threshold at GEO altitudes with two temperature non-extensive electrons. *Space Weather*, *21*, e2022SW003412. https://doi.org/10.1029/2022SW003412

Received 29 DEC 2022
Accepted 6 OCT 2023

Author Contributions:
Conceptualization: Nazish Rubab, Ghulam Jaffer
Methodology: Nazish Rubab
Software: Nazish Rubab
Supervision: Nazish Rubab
Validation: Nazish Rubab
Writing – original draft: Nazish Rubab
Writing – review & editing: Nazish Rubab

1. Introduction

Our space environment has a complicated and dynamic arrangement that can damage the surface and the internal structure of spacecraft. Spacecraft and satellites act as electrical lead in a plasma environment that can accumulate charge particles from the surrounding plasma. The interaction of spacecraft with high-energy space plasmas at such high altitudes can profoundly damage some components of the spacecraft which also affects the functioning of satellites (Harris, 2003; Rubin et al., 1980). In particular, electrostatic discharges can destroy the functionality of spacecraft components thus making them ineffective or inactive (Prokopenko & Laframboise, 1980). It might obstruct telemetry signals and disrupt onboard scientific measurements or electronics (Engelhart et al., 2019).

Numerous investigations have been carried out to study spacecraft surface charging at GEO altitude with inconsistent results. Severe negative spacecraft surface charging can mostly occur when the spacecraft passes through the plasma sheet and is immersed in hot and low-density plasma. The high voltage surface charging has been widely studied through the interplay of spacecraft with the space plasma environment which identifies the strong reliance on plasma parameters such as temperature and number density of particles and space weather conditions (S. T. Lai & Della-Rose, 2001). The observations (Rubin et al., 1980; S. T. Lai, 2012) revealed a critical threshold temperature of electrons and, hence, the failure of devices above this temperature. The critical temperature entirely relies on particle distribution functions, surface properties, and the configuration of space-grade materials. The critical temperature may exist in the range of 1.5–2.5 keV with an average electron temperature between 400 and 3,000 eV in eclipse (S. T. Lai & Della-Rose, 2001; Garrett, 1981), while in sunlight, much

higher temperatures are needed (Mullen et al., 1986). Especially, the data obtained from the Los Alamos National Laboratory geosynchronous (LANL-GEO) satellite revealed the value of a critical temperature in the range of 1–2 keV, which can cause negative charging events with spacecraft potentials as low as −200 V (S. T. Lai & Tautz, 2006). In Geosynchronous orbit, the best correlation with the high-level charging is thus found for electron energies between 10 and 50 keV, which corresponds to an 8 or 9 keV electron temperature threshold (Ferguson et al., 2015). During an eclipse at GEO orbit, the ambient electron current contributes to negative spacecraft potential, particularly when geomagnetic storms and substorms are enhancing the electron flux. On the other hand, when spacecraft are exposed to sunlight the emission of photo-electrons leads to positive charging of a few volts under very low density and temperature conditions which are not usually found in GEO (Pervaiz et al., 2023). A high-level negative charging was also observed in sunlight due to the differential charge, which acts as a potential barrier between surfaces and prevents photo-electrons from escaping on the sunlit side, but to form the barriers to sunlight charging the ambient electron temperature or flux should be very high (Ferguson et al., 2015; Huang et al., 2017).

The GEO satellites ATS 5 and ATS 6 were the first that recorded the extreme charging conditions on the order of −10 kV (DeForest, 1972, 1973) and the SCATHA (Spacecraft Charging at High Altitude) satellite also observed extreme charging events (Craven et al., 1987; Olsen, 1981), which can occur during substorms. When a substorm occurs, there is a sudden injection of energetic hot plasma in the cold plasma environment which forms a relatively low density mixture of hot and cold plasma. Therefore, the geosynchronous plasma being high energy and low density can precisely be modeled by a two-temperatures non-Maxwellian distribution function, where the charging threshold relies on a particle's number density and the temperature of the ambient plasma via the distribution function (S. T. Lai, 2012). In the framework of the two-temperatures distribution space plasma, the onset of spacecraft charging becomes complex since more plasma parameters are involved (S. T. Lai, 1991; Huang et al., 2015). The ambient ion current is omitted for the development of a threshold condition because it measures normally two orders of magnitude smaller than the ambient electron current, especially at GEO altitude. Therefore, due to the greater flux of electrons, the negative surface charging becomes predominant. However, every incoming electron affects the spacecraft material with some energy E that corresponds to outgoing secondary (δ) and back-scattered (η) electrons. The maximum probability of secondary electrons emission (secondary electrons yield) $\delta(E)$ is achieved in the intermediary energy range while back-scattered electrons yield $\eta(E)$ have low energies that are nearly equal to the energy of the incoming electrons (S. T. Lai, 2012). The threshold condition can be achieved when the rate of incoming electrons current is balanced by the outgoing secondary and back-scattered electrons current at a critical temperature and the yield for the two plasma components equals to unity, that is, $\overline{<\delta+\eta>_{c,h}} = 1$.

The space plasmas carry plenty of super-thermal particles and it has been noticed that the statistical properties of charged particles are not governed by a Maxwell-Boltzmann distribution, therefore, it might be well described by a power law distributions. Harris (2003) considered both Maxwellian and anisotropic kappa (Vasyliunas, 1968) distributions to explore the threshold conditions for the onset of significant spacecraft charging at GEO altitude. It was revealed that the kappa distribution better explains the super-thermal charge particles but in the case of low-level charging, the kappa distribution has no significant benefit over Maxwellian. A number of authors have explained that the particle velocity distribution function is often non-Maxwellian (Livadiotis & McComas, 2013) and have successfully employed different approaches such as $q-$ non-extensive distribution (Ali et al., 2020; Pervaiz et al., 2023). The $q-$ non-extensive distribution is better than the kappa distribution as it captures the high energy tail along with the effects of long-range interparticle forces for example, Coulomb forces. In general, the $q-$ non-extensive distribution is better to model both the high-energy tail and the low-energy core of the distribution function and it is also convertible to the non-extensive kappa distribution by the relation $q = 1 \pm \frac{1}{\kappa}$.

In statistical mechanics, the Boltzmann-Gibbs entropy is considered to be extensive when the system holds short-range interparticle forces such as the Vander Waals force and screening or shielding effects (Yoon, 2019), whereas the non-extensivity in the plasma system depends on the long-range interparticle forces. In space plasmas, the charged particles encounter the long-range Coulomb forces, such as the electrostatic force which is responsible for attraction or repulsion that can cause charged particles to scatter when they contact each other over very large distances. The impact of long-range Coulomb scattering can be alleviated due to Debye screening of charged particles causing the ions to form a stationary background in response to an electric field. The free electrons that move in response to the electric field can be well described by Tsallis statistics based on Tsallis entropy ($q-$ parameterized entropy) as long-range forces are limited in space plasma where the region of electron density

is high (Boon & Tsallis, 2005; DeForest, 1972, 1973; Saberian & Esfandyari-Kalejahi, 2014; Safa et al., 2015). The Tsallis entropy (Tsallis, 1988, 1994) is given as

$$S_q = k_B \frac{1 - \sum_i p_i^q}{q - 1},$$

where k_B is the Boltzmann constant and p_i refers to the probability of the system under consideration of microstate configuration, while the index q is a real number that defines the strength of non-extensivity of the system. The unique property of $q-$ statistics or Tsallis entropy is the pseudo-additivity of the composite system $(A + B)$ that is simply composed of two independent subsystems A and B in a manner of factorized microstate probabilities (DeForest, 1973; Tsallis et al., 2005). The Tsallis entropy of a composite system $(A + B)$ can be written as,

$$S_q(A + B) = S_q(A) + S_q(B) + (1 - q)S_q(A)S_q(B).$$

The first component of $S_q(A + B)$ shows the additive property $S_q(A) + S_q(B)$ while the second component is the multiplicative property $(1 - q)S_q(A)S_q(B)$, which includes long-range correlations that support the macroscopic ordering phenomena. In general, q is the parameter that controls the degree of non-extensivity in the framework of statistical mechanics and the term $(1 - q)$ shows how the system deviates from GB statistics to Tsallis statistics. When the non-extensive q-parameter is not equal to unity $(q \neq 1)$, it is referred to as a non-Maxwellian plasma for which the temperature gradient is not equal to zero $(\Delta T \neq 0)$. It should be noted that when the value of the q-parameter is less than unity $(q < 1)$, the entropy of the composite system exceeds the entropy of the independent subsystems $\left[S_q(A + B) > S_q(A) + S_q(B)\right]$, which refers to the super-extensive case. On the contrary, for q greater than unity $(q > 1)$, the entropy of the composite system is less than the entropy of independent subsystems $\left[S_q(A + B) < S_q(A) + S_q(B)\right]$, which refers to sub-extensivity of the system. Moreover, when $q \to 1$, the plasma system becomes Maxwellian and can be defined by the Boltzmann-Gibbs statistics under the condition where $S_q(A + B) = S_q(A) + S_q(B)$, which is clearly not the same as Tsallis entropy. For $q \to 1$, the $q-$ non-extensive distribution reduces to standard Maxwellian distribution (Saberian & Esfandyari-Kalejahi, 2014).

In a recent study (Ali et al., 2020), a comparative analysis was made for the onset of charging at GEO altitude by using different single distribution functions. It was concluded that the $q-$ distribution better supports the charging onset under the limit of super-extensivity $(q < 1)$, as it triggers the charging process faster as compared to Maxwellian and kappa distributions. To model the effects of suprathermal charge particles for significant spacecraft charging at two temperature geosynchronous plasma, we use non-extensive distribution function which is believed to better fit the data with observations.

In the present work, we have revisited the theory of charging onset and threshold conditions at GEO altitude by using the double Maxwellian with two-temperature (Huang et al., 2015) in Section 2 and developed a model to refine the correlation between the spacecraft charging and its interaction with high energy plasma environment based on $q-$ non-extensive distribution function. A modified threshold condition is discussed in Section 3 by using a two-temperature $q-$ non-extensive distribution function within the framework of the Whittaker integral function. Moreover, in Section 4, we have examined the charging currents and various charging behaviors near the threshold for several plasma parametric domains. The criterion of a potential jump is also discussed briefly which predicts the significant conditions for the sudden potential-jump or smooth transition and the stability of a negative potential near the threshold condition in Section 5. Finally, Sections 6 and 7 are devoted for results and discussions and conclusions, respectively.

2. Threshold Condition in Two-Temperature Maxwellian Plasma

The space plasma environment changes with time, altitude and solar activity. In the outer region of GEO, the high-energy plasma clouds comes out of the magnetotail at around midnight hours. The energetic electrons and ions tend to drift eastward and westward, respectively, due to the curvature of the geomagnetic field. As they get closer to the Earth, everything moves eastward because of the co-rotation effect. This happens during "substorm injection," which can more frequently occur during geomagnetic storm activities (S. T. Lai & Della-Rose, 2001; S. T. Lai, 2012). Therefore, the variable plasma at GEO is generated by two plasma sources, the cold plasma (as kT < 10 eV) originating from Earth's ionosphere that can be transported and trapped in GEO orbit through various processes for example, magnetospheric convection, particle precipitation, and the hot plasma accelerated

in substorms. When the energetic hot plasma cloud arrives in GEO where the cold plasma already exists, the plasma distribution may change. As a result, the environment becomes a mixture of two plasmas, having different temperatures (T_c and T_h) and densities (n_c and n_h), where the subscripts c and h refers to two components cold and hot plasma, respectively. The GEO plasma is generally described by a two-temperature Maxwellian distribution which is the sum of low temperature T_c and high temperature T_h component:

$$f(E) = f_c(E) + f_h(E), \tag{1}$$

where

$$f_c(E) = n_c\left(\frac{m}{2\pi k_B T_c}\right)^{\frac{3}{2}} \exp\left(-\frac{E}{k_B T_c}\right), \tag{2}$$

$$f_h(E) = n_h\left(\frac{m}{2\pi k_B T_h}\right)^{\frac{3}{2}} \exp\left(-\frac{E}{k_B T_h}\right). \tag{3}$$

In a single Maxwellian plasma, the threshold condition to trigger surface charging, depends on the critical electron temperature T^* and surface properties of the material, while in the two-temperature scenario, the threshold condition is additionally dependent on the ratio of number densities (n_c/n_h). At the threshold condition, with the assumption that the spacecraft potential is zero, the contribution due to the ions flux can be neglected as the ambient electron current exceeds that of the ambient ions current, therefore, it is necessary that a current balance exists between the flux of incoming electrons and outgoing secondary and back-scattered electrons. In addition, we exclude the photo-electron current because we are looking at the charging phenomenon in eclipse to consider severe charging situation or shaded areas of spacecraft. The current balance equation for two temperature Maxwellian plasma can be transformed as,

$$\int_0^\infty E[f_c(E) + f_h(E)]dE = \int_0^\infty E[f_c(E) + f_h(E)][\delta(E) + \eta(E)]dE, \tag{4}$$

where $\delta(E)$ and $\eta(E)$ are the coefficients of secondary and back-scattered electrons emission, respectively. These coefficients typically depend on the particle's energy and surface properties of the material (S. T. Lai, 2012). The coefficients of secondary and back-scattered electron yields are given as:

$$\delta(E) = c\exp\left(-\frac{E}{a}\right) - c\exp\left(-\frac{E}{b}\right), \tag{5}$$

and

$$\eta(E) = A - B\exp(-EC), \tag{6}$$

where $a(= 4.3E_{\max})$, $b(= 0.367E_{\max})$, and $c(= 1.37\delta_{\max})$ are the constants of surface material and their values have been obtained from observational data (Sanders & Inouye, 1979) where the maximum energy ($E_{\max}$) and yield ($\delta_{\max}$) is dependent on the surface material. The Prokopenko and Laframboise model is used for the back-scattered electrons yield $\eta(E)$, which defines that A, B, and C are function of atomic number (Z) and depend on the surface material properties (Prokopenko & Laframboise, 1980). By substituting Equations 1–3 along with the $\delta(E)$ and $\eta(E)$ coefficients into Equation 4, we eventually get the threshold condition in terms of electron temperature and density (for details see Appendix A)

$$\frac{\alpha(k_B T_c)^{\frac{1}{2}} < \delta + \eta >_c + (k_B T_h)^{\frac{1}{2}} < \delta + \eta >_h}{\alpha(k_B T_c)^{\frac{1}{2}} + (k_B T_h)^{\frac{1}{2}}} = 1. \tag{7}$$

here, α is ratio of number densities, that is, $\alpha = \frac{n_c}{n_h}$, and $< >_{c,h}$denoting the average of the secondary and back-scattered electrons yield in terms of two plasma components (hot and cold), that may be described as:

$$< \delta + \eta >_c = \zeta_\delta(k_B T_c) + \zeta_\eta(k_B T_c),$$
$$< \delta + \eta >_h = \zeta_\delta(k_B T_h) + \zeta_\eta(k_B T_h),$$

where ζ_δ and ζ_η, are the averaged yield of secondary and back-scattered electrons emission, respectively:

$$\zeta_\delta(T_{c,h}) = c\left[\left(1+\frac{k_B T_{c,h}}{a}\right)^{-2} - \left(1+\frac{k_B T_{c,h}}{b}\right)^{-2}\right],$$
$$\zeta_\eta(T_{c,h}) = A - B(1+Ck_B T_{c,h})^{-2}.$$

Equation 7 gives the threshold condition for the onset of the spacecraft charging that depends on surface material properties and electron temperatures and densities and is only valid for spacecraft charging in eclipse where the contribution due to photo-electrons is ignored (S. T. Lai, 2012; Huang et al., 2015).

3. The Threshold Conditions in a Two Temperature q − Non-Extensive Distribution Function

In GEO environment, the energetic particle injection associated with substorms contribute a supply of new particle populations in the range of hundreds of keV. In such scenario, the presence of high energy particles can be well described by a two- temperature q − non-extensive distribution, which gives a better fit to the data in space plasma environment. In order to display the threshold condition, the current balance equation has been analyzed in eclipse and we discussed the impact of the two-temperature non-extensive distribution by using the Whittaker function approach. A Whittaker function is a special solution of Whittaker's equation, that is a modified form of the well-known confluent hypergeometric equation (Chaudhry & Zubair, 1992; Dereziński & Richard, 2018). This approach serves less error in the numerical solution and converges more quickly to the Maxwellian (Morse & Feshbach, 1953) as shown in our graphical representation. The generalized 3-D q − non-extensive energy distribution function is,

$$f_e(E) = B_q \frac{n_e}{(k_B T_e)^{\frac{3}{2}}}\left(1-(q-1)\frac{E}{k_B T_e}\right)^{\frac{1}{q-1}}, \tag{8}$$

where, k_B is Boltzmann constant and T_e, n_e are the electron temperature and number density, while B_q is a normalized constant defined as (Appendix A)

$$B_q = \frac{\Gamma\left(\frac{1}{1-q}\right)(1-q)^{\frac{3}{2}}\left(\frac{m}{2\pi}\right)^{\frac{3}{2}}}{\Gamma\left(\frac{1}{1-q}-\frac{3}{2}\right)}, \text{ for } -1<q<1,$$
$$B_q = \frac{(3q-1)(q-1)^{\frac{3}{2}}\Gamma\left(\frac{1}{q-1}+\frac{3}{2}\right)\left(\frac{m}{2\pi}\right)^{\frac{3}{2}}}{2\Gamma\left(\frac{1}{q-1}\right)}, \text{ for } q>1 \tag{9}$$

The non-extensive q-parameter can be revealed by fitting the distribution to observed data and provides a useful tool for exploring the various physical phenomena at space plasmas. It is characterized by the fraction of non-thermal particle components that control the degree of non-extensivity in the framework of statistical mechanics, indicating the effect of long-range interactions in the system. In the limiting case ($q \to 1$), the q − non-extensive distribution reduces to the generalized Maxwell Boltzmann distribution function. For $q \neq 1$, the distribution represents the non-extensivity of the particles, whereas $q<1$ and $q>1$ lead to the super-extensive and sub-extensive cases, respectively.

The non-extensive behavior of the q − non-extensive distribution at different values of q is shown in Figure 1. It is clear from the limit of sub-extensivity ($q>1$) that the low probabilities of the distribution function are depressed and high probabilities are increased as compared to Maxwellian distribution. Therefore, this limit is suitable to explain the plasma system containing the low energy particles as they capture the low-energy core of the distribution function. Whereas in the limit of super-extensivity ($q<1$), the q − non-extensive distribution behaves like the kappa distribution function (Vasyliunas, 1968) as they capture the super-thermal charge particles at low probabilities as compared to Maxwellian distribution. When hot energetic solar wind plasma is injected into Geosynchronous orbit, the resulting plasma is a combination of two plasmas with different electron temperatures (T_c and T_h) and number densities (n_c and n_h). Therefore, Equation 8 will take the form

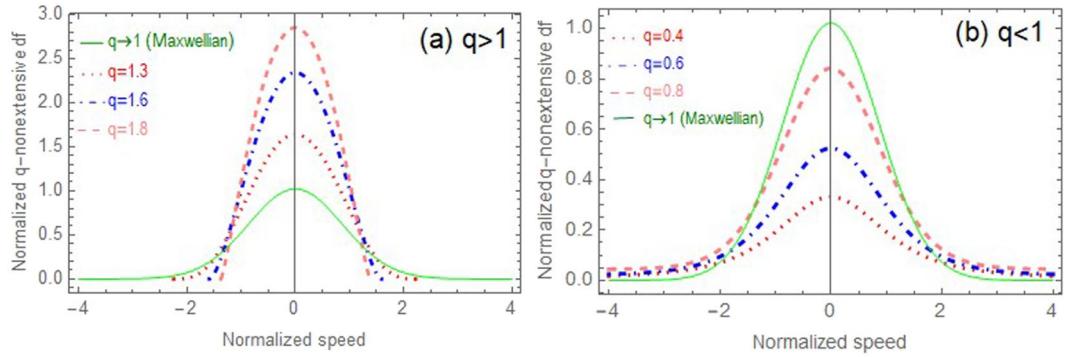

Figure 1. The non-extensive behavior of the $q-$ non-extensive distribution function.

$$f_q(E) = B_q \left[\begin{array}{l} \frac{n_c}{(k_B T_c)^{\frac{3}{2}}} \left(1 - (q-1)\frac{E}{k_B T_c}\right)^{\frac{1}{q-1}} + \\ \frac{n_h}{(k_B T_h)^{\frac{3}{2}}} \left(1 - (q-1)\frac{E}{k_B T_h}\right)^{\frac{1}{q-1}} \end{array} \right]. \tag{10}$$

Substituting Equations 5, 6, and 10 into Equation 4, the current balance equation turns out to be

$$\frac{\begin{array}{l} \alpha(k_B T_c)^{\frac{1}{2}} \left[c(U_1 - U_2)_{T_c} + A\frac{(1-q)^2}{2q^2 - q} - B(U_3)_{T_c} \right] \\ +(k_B T_h)^{\frac{1}{2}} \left[c(U_1 - U_2)_{T_h} + A\frac{(1-q)^2}{2q^2 - q} - B(U_3)_{T_h} \right] \end{array}}{\frac{(1-q)^2}{2q^2-q}\left[\alpha(k_B T_c)^{\frac{1}{2}} + (k_B T_h)^{\frac{1}{2}}\right]} = 1, \tag{11}$$

where $\alpha(= n_c/n_h)$ is the ratio of number densities, $(U_1, U_2, U_3)_{T_{c,h}}$ are the hypergeometric functions associated with T_c and T_h in Equation 11 reading

$$\begin{aligned} (U_1)_{T_{c,h}} &= U_1\left(2\left|3 + \frac{1}{q-1}\right|\frac{k_B T_{c,h}}{(1-q)a}\right), \\ (U_2)_{T_{c,h}} &= U_2\left(2\left|3 + \frac{1}{q-1}\right|\frac{k_B T_{c,h}}{(1-q)b}\right), \\ (U_3)_{T_{c,h}} &= U_3\left(2\left|3 + \frac{1}{q-1}\right|\frac{C\, k_B T_{c,h}}{(1-q)}\right). \end{aligned}$$

After simplification, Equation 11 can also be expressed as

$$\frac{\alpha(k_B T_c)^{\frac{1}{2}}[<\delta + \eta>_c] + (k_B T_h)^{\frac{1}{2}}[<\delta + \eta>_h]}{\frac{(1-q)^2}{2q^2-q}\left[\alpha(k_B T_c)^{\frac{1}{2}} + (k_B T_h)^{\frac{1}{2}}\right]} = 1, \tag{12}$$

Which is the modified current balance equation in a two temperature $q-$ non-extensive plasma. Here, $<\delta + \eta>_{c,h}$ is the average secondary and back-scattered electron yield for two plasma components T_c and T_h whose values are now dependent on the non-extensive $q-$ parameter given by,

$$\begin{aligned} <\delta + \eta>_c &= c(U_1 - U_2)_{T_c} + A\frac{(1-q)^2}{2q^2 - q} - B(U_3)_{T_c}, \\ <\delta + \eta>_h &= c(U_1 - U_2)_{T_h} + A\frac{(1-q)^2}{2q^2 - q} - B(U_3)_{T_h}. \end{aligned}$$

Table 1
Critical T and Anti-Critical Temperature T* of Different Material (Given in keV) With Maxwellian and q − Non-Extensive Distribution*

Material	Maxwellian		q − non-extensive			
			q > 1		q < 1	
	T*	T_A	T*	T_A	T*	T_A
CuBe	1.4	0.020	1.8	0.73	0.92	0.016
Gold	2.9	0.114	ε	ε	0.07	2
SiO_2	1.7	0.029	2.5	1.98	0.64	0.022
Kapton	0.5	0.014	Indeterminate	Indeterminate	ε	ε
Al oxide	1.2	0.020	2.4	0.99	0.45	0.015
Teflon	1.4	0.017	Indeterminate	Indeterminate	0.54	0.017
Mg oxide	2.7	0.016	4.1	1.61	1.15	0.009
Silver	1.2	0.315	ε	ε	ε	ε
Glass	1.4	0.015	2.6	1.4	0.53	0.022
Mg	ε	ε	ε	ε	ε	ε
Indium oxide	2.0	0.108	ε	ε	1.3	0.07
MgF_2	7.8	–	6	–	ε	ε
Al	ε	ε	ε	ε	ε	ε

Note. Where, ε indicates that the average yield of secondary and back-scattered electrons $<\delta+\eta>_{c,h}$ is below than unity and empty columns show that there is no anti-critical temperature T_A associated to that material.

The modified threshold condition Equation 12, is the weighted average over the total secondary and back-scattered electron yields and equals to unity $\overline{<\delta+\eta>_{c,h}}=1$, accounted by the two-temperature q − non-extensive energy distribution function. The current balance equation is developed with the help of the Whittaker function which is commonly used to describe charging related problems (Harris, 2003; Morse & Feshbach, 1953; Pervaiz et al., 2023). Equation 12 is valid for spacecraft charging in eclipse and in the limit $T_h=0$, we obtain the expression for the single temperature q − non-extensive case (Ali et al., 2020), that is,

$$\frac{2q^2-q}{1-q}\{cU_1-cU_2-BU_3\}+A-1=0. \tag{13}$$

In the limit $(q\to 1)$, the threshold conditions expressed in Equations 12 and 13 approach to the Maxwellian distribution. The numerically calculated values of the critical temperature T^* and anti-critical temperature T_A of various surface materials obtained from Equations 7 and 12, are given in Table 1. The anti-critical temperature T_A refers to the minimum amount of energy at which the average yield of secondary and back-scattered electrons emission equals to unity (S. Lai & Tautz, 2008).

4. Charging Behavior at the Threshold Condition

To calculate the charging levels or charging behavior in non-Maxwellian plasma, the electron fluxes play a dominant role. The charging current of a spherical spacecraft is represented by the following equation:

$$I(\phi)=4\pi h^2 e_j\int_{-\infty}^{\infty}\vec{v}\,f\left(\vec{v}\right)d^3\vec{v}, \tag{14}$$

where, $h=a\left(1-\frac{e_j\phi}{KT}\right)^{\frac{1}{2}}$ is the distance measured from the center of sphere to the straight line of travel, $\vec{v}$ is particle velocity touching the spacecraft tangentially at $a=r$ and $e_j=z_j e$ is the elementary charge where j stands for $i=ions$ and $e=electrons$, respectively. The following relation has been derived in order to calculate the flux or current density at any point on the surface of a spacecraft,

$$J=e_j\frac{2\pi}{m_j^2}\int_{E_{\min}}^{E_{\max}}(E-e_j\phi)f(E)dE, \tag{15}$$

where $f(E)$ is the particles energy distribution function. To elucidate Equation 15 with q − non-extensive distribution function, we arrive at,

$$J=\left\{\begin{array}{c} B_q e_j\frac{2\pi}{m_j^2}\frac{n_e}{(k_B T_j)^{\frac{3}{2}}}\int_{E_{\min}}^{\infty}(E-e_j\phi)\left(1-(q-1)\frac{E}{k_B T_j}\right)^{\frac{1}{q-1}}dE \\ \text{for}\quad -1<q<1 \\ B_q e_j\frac{2\pi}{m_j^2}\frac{n_e}{(k_B Tj)^{\frac{3}{2}}}\int_{E_{\min}}^{E_{\max}}(E-e_j\phi)\left(1-(q-1)\frac{E}{k_B T_j}\right)^{\frac{1}{q-1}}dE \\ \text{for}\quad q>1 \end{array}\right\}. \tag{16}$$

After performing the integration on Equation 16, we can obtain a simplified form of current density in non-extensive plasma

$$J=J_0\frac{L_q}{2q^2-q}\exp\left(-\frac{e_j\phi}{k_B T_j}*\frac{2q^2-q}{q}\right). \tag{17}$$

Here, $J_0 = n_j e_j \left(\frac{k_B T_j}{2\pi m_j}\right)^{\frac{1}{2}}$ and L_q is a function of the q parameter given by,

$$L_q = \begin{Bmatrix} \frac{\Gamma\left(\frac{1}{1-q}\right)(1-q)^{\frac{3}{2}}}{\Gamma\left(\frac{1}{1-q}-\frac{3}{2}\right)} & \text{for} \quad -1 < q < 1 \\ \frac{(3q-1)(q-1)^{\frac{3}{2}}\Gamma\left(\frac{1}{q-1}+\frac{3}{2}\right)}{\Gamma\left(\frac{1}{q-1}\right)} & \text{for} \quad q > 1 \end{Bmatrix}.$$

The parameter q stands for the non-extensivity of the plasma species and Γ denotes the standard Gamma function. For analytical investigations of charging behavior near the threshold, the total charging flux on the spacecraft in eclipse can be described as follows:

$$\begin{aligned} J_T(\phi) = {} & J_{ic}(0)\frac{L_q}{2q^2-q}(1+Q) + J_{ih}(0)\frac{L_q}{2q^2-q}(1+Q) \\ & - J_{ec}(0)\frac{L_q}{2q^2-q}\exp(-Q)(1-<\delta+\eta>_c) \\ & - J_{eh}(0)\frac{L_q}{2q^2-q}\exp(-Q)(1-<\delta+\eta>_h), \quad \text{for} \quad \phi < 0 \end{aligned} \tag{18}$$

where $J_T(\phi)$ is the total charging flux with the contribution of two-temperature plasma species and $Q = \frac{e_j|\phi|}{k_B T}\left(\frac{2q^2-q}{q}\right)$. The above charging equations includes the effect of electrons as well as ions for careful investigations of potential variations, while the ion's contribution was neglected in the current balance equation due to the equilibrium potential at the threshold.

5. General Conditions for Potential Jump at Threshold

In a two-temperature non-extensive plasma, the onset of charging becomes complex due to many parameters involved and multiple roots may exist for current balance equation. Moreover, the spacecraft potential can occur in different ways: it can transit smoothly or suddenly jump at some stable negative values. However, the reason of the potential jump from one potential to another potential is the fact that transitional states are not stable. The stability of the threshold solution may be determined by $\frac{dJ}{d\phi}$, according to Whipple (1981), the potential is only stable when $\frac{dJ}{d\phi} < 0$. From Equation 18, the stability of the negative potential near the threshold in non-extensive two-temperature plasma can be obtained:

$$\frac{dJ_T(\phi)}{d\phi} = -n_h e_j \begin{Bmatrix} \sqrt{\frac{m_e}{m_i}}\frac{L_q}{2q^2-q}\left(\frac{2q^2-q}{q}\right)\left(\frac{\alpha}{\sqrt{k_B T_c}} + \frac{1}{\sqrt{k_B T_h}}\right) \\ +\frac{L_q}{2q^2-q}\left(\frac{2q^2-q}{q}\right)(1-<\delta+\eta>_1)\alpha\sqrt{k_B T_c} \\ \left[\frac{1}{k_B T_c}\exp\left(\frac{e_j\phi}{k_B T_c} * \frac{2q^2-q}{q}\right) - \right. \\ \left. \frac{1}{k_B T_h}\exp\left(\frac{e_j\phi}{k_B T_h} * \frac{2q^2-q}{q}\right)\right] \end{Bmatrix} \text{for } \phi < 0. \tag{19}$$

We can observe the charging on the surface of the satellite due to the variation of current density. We have used Equation 12 in Equation 19 to evaluate the potential near the threshold. It is instructive to note that the RHS of Equation 19 is negative and in order to achieve a stable solution, the following conditions has to be satisfied:

$$\zeta(\phi) < C_o \quad \text{for} \quad <\delta+\eta>_c > 1, \tag{20}$$

$$\zeta(\phi) > C_o \quad \text{for} \quad <\delta+\eta>_c < 1, \tag{21}$$

where

$$\zeta(\phi) = \frac{1}{k_B T_c}\exp\left(\frac{e_j\phi}{k_B T_c} * \frac{2q^2-q}{q}\right) - \frac{1}{k_B T_h}\exp\left(\frac{e_j\phi}{k_B T_h} * \frac{2q^2-q}{q}\right), \tag{22}$$

and

$$C_o = \frac{\sqrt{\frac{m_e}{m_i}}\left(\frac{\alpha}{\sqrt{k_B T_c}} + \frac{1}{\sqrt{k_B T_h}}\right)}{(<\delta + \eta>_c - 1)\alpha\sqrt{k_B T_c}}. \tag{23}$$

6. Results and Discussion

The Geosynchronous plasma is usually better modeled by two-temperature plasma especially in a substorm scenario when energetic particles are injected in a tenuous and cool GEO plasma. The energized plasma particles impacting the spacecraft surface are described by using two-temperature non-Maxwellian plasma. In such a framework, the onset of charging becomes complicated since a number of parameters, that is, average yields $<\delta + \eta>_{c,h}$, non-extensivity ($q \lesseqgtr 1$), density population ratio (n_c/n_h) and the temperatures (T_c and T_h) of hot to cold non-extensive electrons are involved. The current balance equation is modeled to investigate the onset of significant surface charging due to secondary and back-scattered electrons and to determine the critical temperature for various space-grade materials by employing the $q-$ non-extensive distribution. Since surface charging is the main focus in spacecraft component design and simulations, it is necessary to determine the impact of secondary and back-scattered electrons yields on various materials as it not only depends on the surface conditions but also on the energy distribution of primary charged particles (S. T. Lai, 2010; Ali et al., 2020). The behavior of the distribution function for $q \lesseqgtr 1$ is depicted in Figures 1a and 1b which indicates that for $q > 1$, the q-distribution exhibits the thermal cutoff at the maximum energy value allowed for the charge particles given by $E_{\max} = k_B T_f/(q-1)$, while the value of the lower limit of the integral is $E_{\min} = 0$. It is clearly demonstrated that the $q-$ non-extensive distribution reduces to the Maxwellian distribution when the strength of the non-extensivity q approaches to unity. To analyze the charging onset in two-temperature plasma, the weighted average over the total secondary and back-scattered electron yields should be equal to unity, that is, $<\delta + \eta>_{c,h} = 1$. Based on the current balance equation for two-temperature Maxwellian and non-extensive distribution functions, we get numerical values of the critical and anti-critical temperatures for various surface materials that are listed in Table 1. The critical and anti-critical temperature are the points where the average total yields cross unity. At high temperatures, the incoming electron flux is balanced by the outgoing flux, and the temperature where the balance occurs is called the critical temperature T^*. It is worth noting that T_A appears as a second solution at a lower temperature that charges the surface to a negative voltage below T_A, but is prevented above it. Interestingly, the values for the critical temperature T^* obtained for the single and double Maxwellian cases remain same, but they reduce significantly when we employ $q-$ non-extensive distribution function. These numerical values show that the significant negative charging due to $q-$ non-extensive plasma triggers the charging process earlier (case $q < 1$) as compared to Maxwellian plasma.

We numerically analyzed the average electron yields for various surface materials as a function of the electron temperature to observe the behavior of two-temperature $q-$ non-extensive distribution while keeping the density ratio α and T_h fixed. Figures 2a–2d are the graphical representation of finding the roots of the current balance equation and to determine the threshold energies for Aluminum oxide (Al_2O_3) and Teflon. We choose typical parametric values for Al_2O_3, that is, $E_{\max} = 0.30$ keV, $\delta_{\max} = 2.60$, $A = 0.1238$, $B = 0.0172$, $C = 0.3455$ (S. T. Lai, 2012) and it is clear [from Figure 2a] that at the high temperatures, the curve associated with the average electron yield goes below unity, which contributes in significant negative charging. The point where the curve cuts unity is the critical temperature T^*, while at low temperatures the unity crossing point is the anti-critical temperature T_A. The $q-$ non-extensive yield curve in the limit $q < 1$, goes below unity earlier than for the Maxwellian curve, as they capture the energetic electrons at low probabilities and we get $T^* = 0.45$ and $T_A = 0.013$, which shows that Aluminum oxide can initiate the charging process faster in non-extensive space plasma. For the limit $q > 1$, as shown in Figure 2b, the critical and anti-critical temperatures are ($T^* = 2.4$ keV and $T_A = 0.99$ keV), the $q-$ non-extensive distribution triggers charging slower than Maxwellian due to the fact that high probabilities are increased at lower energy states as compared to the Maxwellian curve (Black solid line). It should be noted that when we change the constant values of T_h and α, the critical temperature is also changed because the spacecraft charging onset is dependent on the temperature and density of the ambient plasma while in single temperature plasma, density plays no role.

Similarly for Teflon, $E_{\max} = 0.30$ keV, $\delta_{\max} = 3.00$, $A = 0.09$, $B = 0.0$, and $C = 0.0$ (S. T. Lai, 2012), we have again analyzed the charging onset as depicted in Figure 2c. For $q < 1$, the average secondary and back-scattered

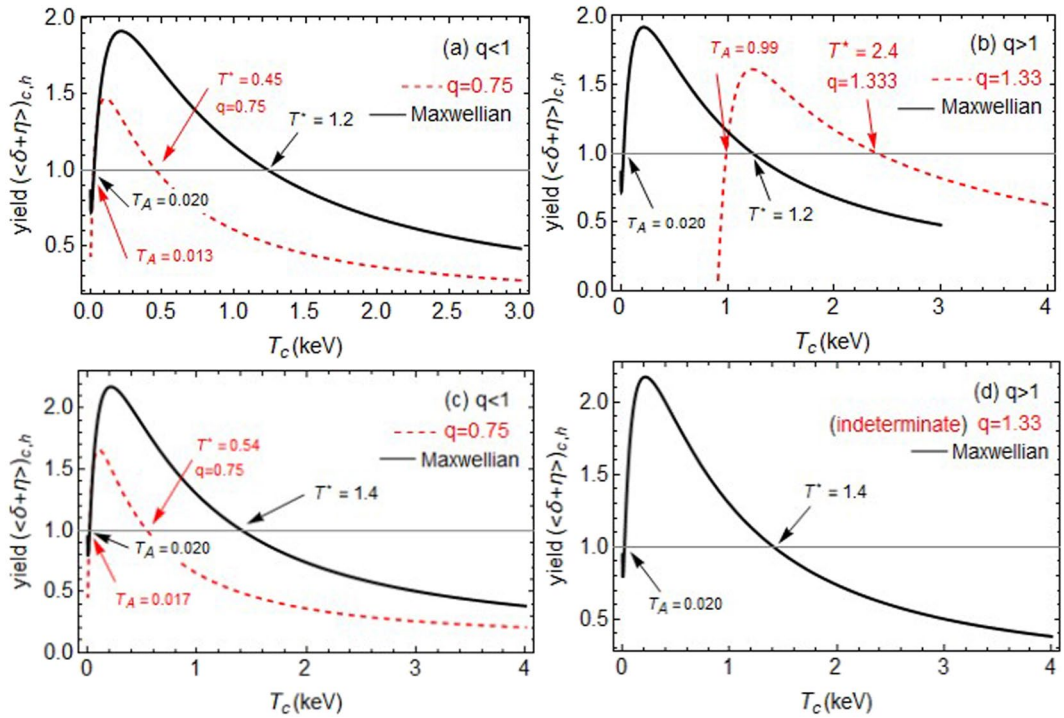

Figure 2. The average secondary and back scattered electron yield is plotted against the electron temperature T_c at a constant density ratio ($\alpha = 7$) and temperature ($T_h = 1.5$ keV). For both limits, the value of q is different, the black solid curve represent the Maxwellian yield while dotted curve shows the non-extensive yield for two temperatures onset of surface charging. Panels (a) and (b) correspond to the surface material Aluminum oxide and (c), (d) represents Teflon.

electron yield $<\delta + \eta>_{c,h}$ cross unity at the points ($T^* = 0.54$ keV and $T_A = 0.017$ keV) and triggers the charging process earlier than the Maxwellian but in the limit $q > 1$, the charging level of the surface material corresponding to Teflon is not precisely fixed. Hence, the onset surface charging leads to Maxwellian plasma, as illustrated in Figure 2d. However, $q > 1$ is suitable to explain the space plasmas at low altitudes containing the low energy particles, as it identifies low probabilities at high energy states. For a further comparison with space grade materials, like silver (Ag), Magnesium (Mg), Magnesium oxide (MgO_2), and CuBe etc., we observed that the silver material with surface properties $E_{max} = 0.80$ keV, $\delta_{max} = 1.00$, $A = 0.3900$, $B = 0.2890$ and $C = 0.6320$, is unable to trigger charging at low temperatures and acquires higher anti-critical temperature T_A due to the higher values for E_{max} and the near unity value for δ_{max}. The yield curves are below unity under both the limits $q < 1$ or $q > 1$, and it will be charged in Maxwellian plasma displayed in Figures 3a and 3b.

The steady potential at which a spacecraft is charged, depends on the plasma environment as well as on the surface conditions of the material and it must be the solution of the current balance equation, that is, $I_{net}(\varphi) = 0$. To determine the charging onset, it is important to measure the current and potential on the spacecraft surface. Therefore, we have numerically elucidated the behavior of the current by using a two-temperature $q-$ non-extensive distribution and by choosing various space grade materials to determine the potential characteristics. First, the normalized currents have been plotted as a function of temperature T_c for a number of materials, while T_h and α are kept constant. In the limiting case of super-extensivity ($q < 1$), the generalized $q-$ non-extensive distribution leads to initiate the onset charging process of spacecraft as compared to Maxwellian distribution and for $q \to 1$, the non-extensive curve of normalized current is approaching to the Maxwellian curve. However, in determining the spacecraft charging current under the limit of sub-extensivity ($q > 1$) we identified the high probabilities that are associated with the suprathermal particles at lower energy states, and the Maxwellian distribution plays a dominant role in the charging onset. To examine the impact of high-energy particles on the charging onset, we also found the low magnitude currents, as an example in Figures 4 and 5, the trend is shown for CuBe and Silver. We, therefore, conclude that for $q < 1$, the generalized $q-$ non-extensive distribution plays a dominant role in the charging onset while, in the limit $q > 1$, the high energy particles cannot be captured, and in that case, the Maxwellian distribution leads to initiate the charging process. Second, we have also plotted the current that varies

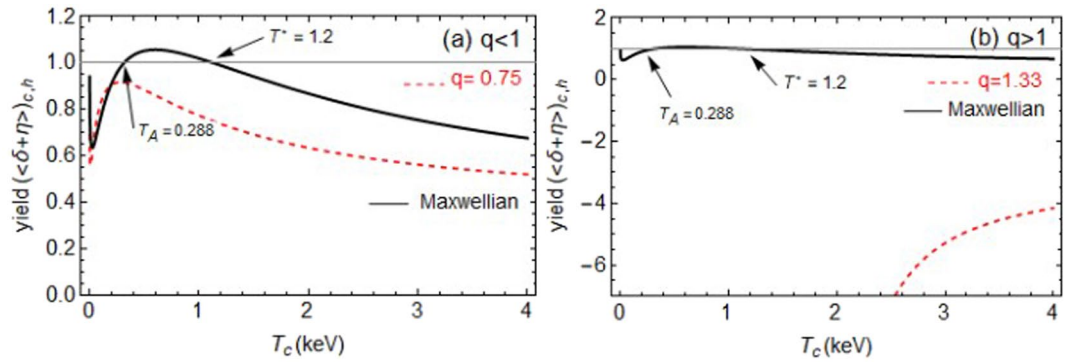

Figure 3. The average secondary and back scattered electron yield is plotted against the electron temperature T_c at a constant density ratio ($\alpha = 7$) and temperature ($T_h = 1.5$ keV). For both limits, the value of q is different, the black solid curve represent the Maxwellian yield while dotted curve shows the non-extensive yield for two temperatures onset of surface charging. Panels (a) and (b) correspond to the surface material silver (Ag).

at the surface of spacecraft as a function of the potential to determine the impact of high energy plasma particles on surface charging. The flux-voltage plot is illustrated in Figures 6a and 6b, in which the curves for positive and negative potential are drawn, which shows that the electrons potential increases with increasing current density for both Maxwellian and non-extensive plasma. In the non-extensive case, it is clear from Figure 6b that at large values of the q parameter, the potential is decreasing, while for ions, the potential is increasing at large values of q. The non-extensive curve reaches to the Maxwellian under the limit $q \to 1$.

The space plasma environment is critical for spacecraft charging analysis due to high and low solar activities and variability of density and energy. It has been noticed, that during the substorms, the onset of significant surface charging of the spacecraft at GEO altitudes is about tens of thousands of eV due to the sudden injections of high-energy plasma particles from magnetotail, and the parameters of GEO plasma will generally fall in the domain $T_A < T_c < T^* < T_h$, which is the requirement of a steady state solution so that the potential transition always takes place at the threshold. We have also investigated different charging behaviors at the threshold condition to describe the impact of low and high energy particles on charging onset at GEO altitudes, especially during a substorm. To examine the charging behavior at a parametric domain, the threshold conditions and the average secondary and back-scattered electron coefficients corresponds to CuBe are illustrated in Figure 7. By varying the temperature T_c and density ratio α at a fixed $T_h = 28$ keV, the average secondary and back-scattered electron yield $<\delta + \eta>_{c,h}$ has been plotted for comparison and it is observed that T_A(=0.009 keV), T^*(=2.4 keV) for Maxwellian and T_A(=0.010 keV), T^*(=0.91 keV) for $q-$ non-extensive for the limit $q < 1$. The anti-critical temperature refers the low voltage and low temperature surface charging due to ambient electrons and are observed to be very close for both distribution while, T_A(=0.73 keV), T^*(=1.8 keV) for the limit $q > 1$. The threshold condition of both $q-$ non-extensive and Maxwellian falls between the range of T_A and T^*, while above the region $<\delta + \eta>_{c,h} > 1$ the low positive charging can occur and below the region $<\delta + \eta>_{c,h} < 1$, extreme negative spacecraft charging

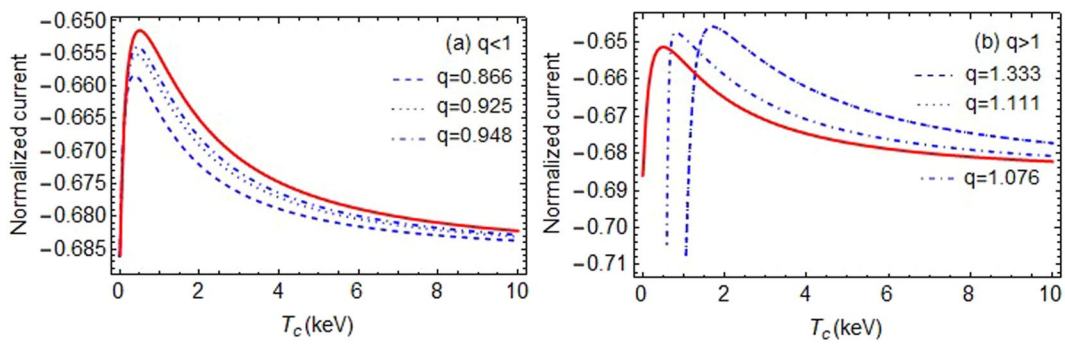

Figure 4. Normalized current as a function of electron temperature T_c while T_h(=100 keV) and α(=0.35) are kept constant shown for different values of q and the Maxwellian curve represented as (solid red curve). Panels (a) and (b) correspond to the surface material CuBe.

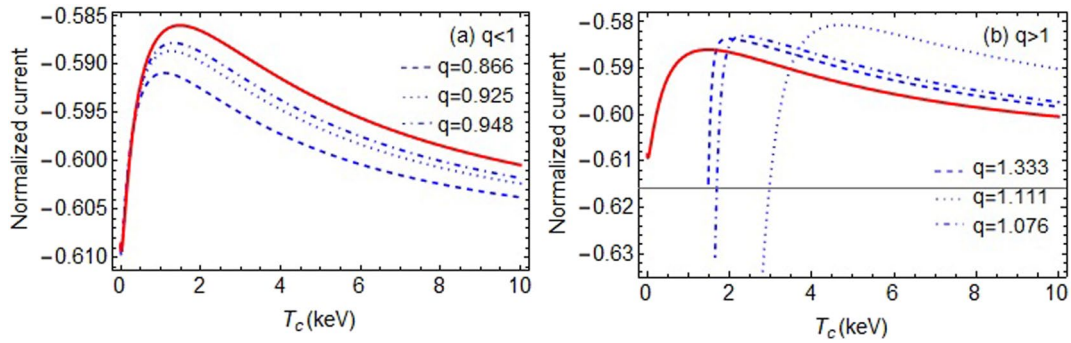

Figure 5. Normalized current as a function of electron temperature T_c while T_h(=100 keV) and α(=0.35) are kept constant shown for different values of q and the Maxwellian curve represented as (solid red curve). Panels (a) and (b) correspond to the surface material Silver (Ag).

take place. It is clear from Figure 7a, that when the threshold condition satisfies $T^* < T_h$, the total electron flux relative to T_c is outgoing and falls between the range of T_A and T^*, and the impact of the $q-$ non-extensive distribution on the threshold condition is more clear under the limit $q < 1$, as it captures the non-extensive particles and initiates the charging process quickly. It can be analyzed that $q > 1$ is still more significant for low energized particles than Maxwellian, therefore, the Maxwellian distribution takes a dominant role to trigger charging which is displayed in Figure 7b. Since the spacecraft potential is positive above the threshold $<\delta + \eta>_{c,h} > 1$ when $T_c < T^*$, it should be negative below the threshold $<\delta + \eta>_{c,h} < 1$ during $T^* < T_h$, as the change in onset spacecraft surface potential from negative to positive or vise versa, it must have to pass through the zero potential value (at threshold condition).

From the charging Equation 18 at the extreme negative surface potential, the magnitude of $\phi < 0$ increases and the total incoming flux gives rise to a positive value, therefore, the ion's flux can dominate the electron's flux. There are certain cases for onset surface potential of spacecraft from being negative to being positive potential that depend on the parametric domain of GEO plasma. For $T_A < T_c < T^* < T_h$, the spacecraft potential transit smoothly from positive potential to the negative potential and that have must pass to the zero potential value while crossing the threshold condition for $T_c < T_A < T_h < T^*$, the spacecraft potential can jump suddenly from a positive potential value to some stable negative potential. In counting the spacecraft potential during the substorm when $T_h > T^*$, we observe the potential evolution by the variation of both potential and density ratio α at fixed temperatures T_c(=0.04 keV) and T_h(=28 keV) and found that the onset surface potential of spacecraft suddenly jump from positive potential to some stable value of negative potential as shown in Figure 8. It is also observed from the series of different charging levels denoted by 1–3 from Figure 7a that helps to illustrate the evolution of potential history. It has been noticed that the potential jump occur in both Maxwellian and non-extensive plasma is according to their threshold condition. The charging level at point 1 represent the region $<\delta + \eta>_{c,h} > 1$, where the spacecraft potential is positive while the point 2 represent the threshold condition $<\delta + \eta>_{c,h} = 1$, where there

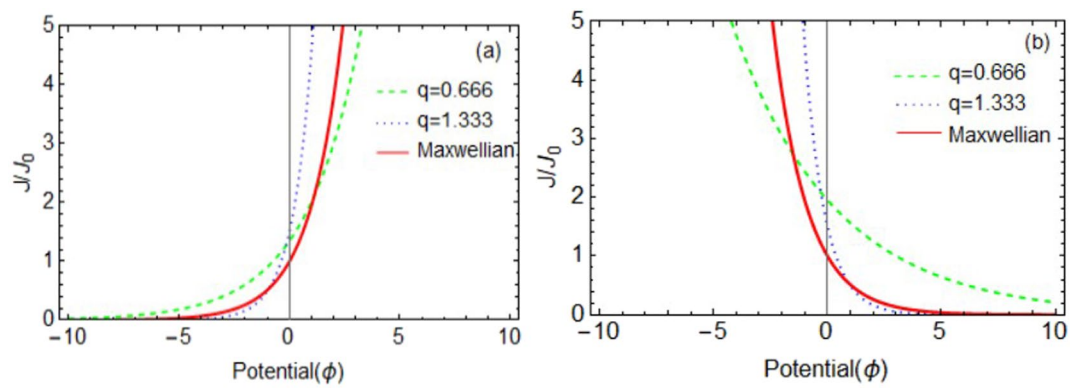

Figure 6. The current is plotted against the potential for different values of q. (a) The electron current; (b) the ion current.

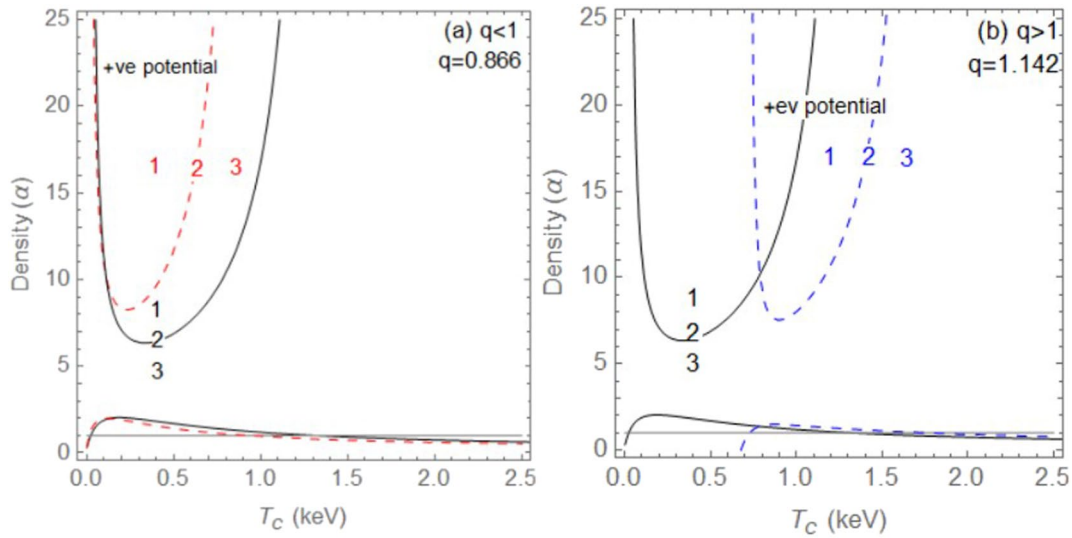

Figure 7. The threshold condition and average secondary and back scattered yield for CuBe. The dashed line represent the $q-$ non-extensive threshold condition and the solid line represent Maxwellian threshold for plasma parametric domain $T_A < T_c < T^* < T_h$.

is a balance between the rate of incoming and outgoing flux and at that point the spacecraft potential is equal to zero. The point 3 shows the negative potential at $<\delta + \eta>_{c,h} < 1$.

At the same time, the space plasma at GEO altitude also contains low-energy electrons (typically a few eV) clouds. The Low energy electrons generally with $T_c < T_A$, trap around the spacecraft, especially in case of differential charging. In such a situation the plasma parametric domain falls in the range of $T_c < T_A < T_h < T^*$. Both Maxwellian and $q-$ non-extensive threshold conditions are plotted for this domain using CuBe surface material at fixed T_h(=0.5 keV), the result shows the two branches of threshold that appeared in the range $T_c < T_A$ and $T_c > T^*$ [see Figure 9] means above the threshold condition or inside both branches the spacecraft is negatively charged and below the threshold it becomes positively charged. We observed that when the threshold satisfies the given condition $T_A < T_h < T^*$, the total electron flux is outgoing because of the second component of plasma T_h. To balance the outgoing electron flux, the first plasma component can generate the incoming electron flux only when it falls in the range $T^* < T_c < T_A$. For the limit $q < 1$, the $q-$ non-extensive threshold condition [see Figure 9a] in the range $T_c < T_A$ and $T_c > T^*$ can initiate the onset of negative surface charging of the spacecraft in comparison with Maxwellian and for $q > 1$, from [Figure 9b] the impact of $q-$ parameter is obvious but the Maxwellian distribution takes the effective lead in onset surface charging and in the region $T_c < T_A$, the threshold

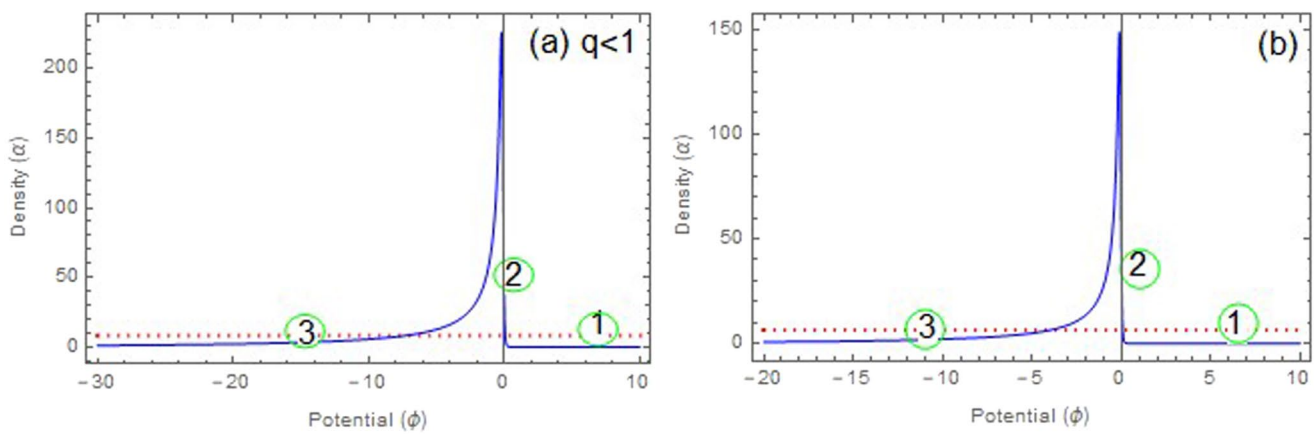

Figure 8. The variation of potential with density ratio for $T_A < T_c < T^* < T_h$ plasma parametric domain, (a) represent q -non-extensive potential jump with $q = 0.857$, and (b) Maxwellian.

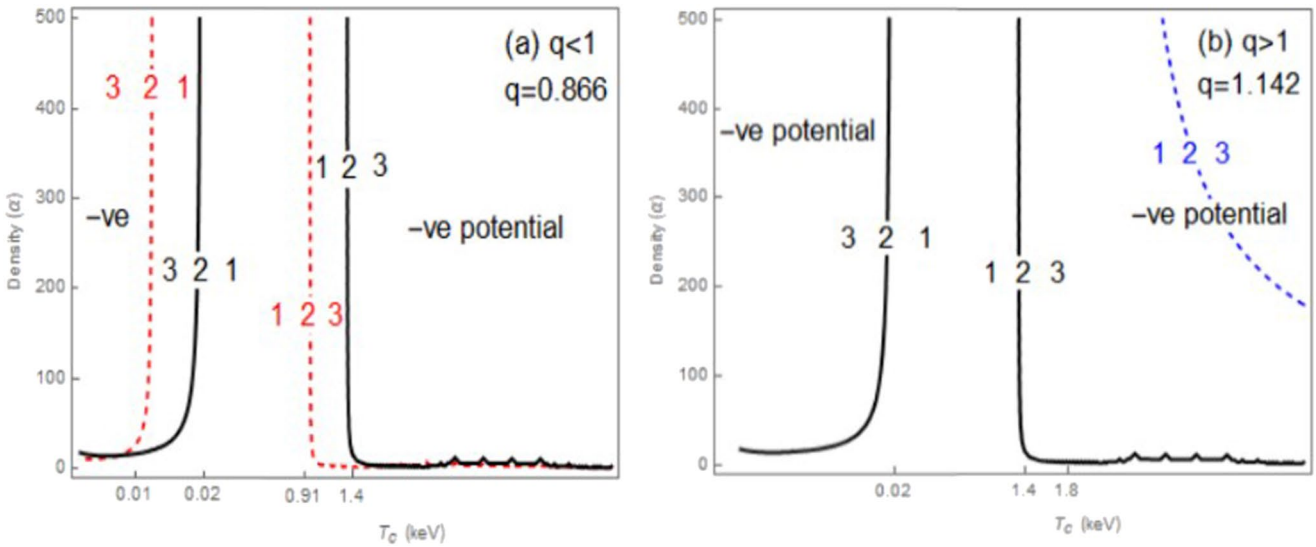

Figure 9. The threshold condition for CuBe, dashed line (q-non-extensive) and solid line (Maxwellian) threshold condition for plasma parametric domain $T_c < T_A < T_h < T^*$.

curve is not found due the fact that the number of electron associated with the charging onset in non-extensive plasma is very small for the sub-extensive state $q > 1$. For the plasma parametric domain $T_c < T_A < T_h < T^*$, the evolution of potential has been illustrated as the variation of density ratio at constant temperatures T_c(=0.003 keV) and T_h(=0.5 keV) in Figure 10, along with the different charging levels as explained previously, denoted by 1–3 from [Figure 9a] the potential curve can transits smoothly from some positive potential value to the negative value in both non-extensive and Maxwellian plasma when their threshold condition is approached.

For space plasmas, it is quite clear to see that the Maxwellian distribution function can give accurate results for low-energy particles but it does not describe the actual plasma situation at or near the geosynchronous Earth orbit, due to the presence of high energy particles especially when two-temperature plasma is present at such altitude. Therefore, the $q-$ non-extensive distribution gives more generalized results in modeling the suprathermal particles in space plasmas, especially within the limit of super-extensivity $q < 1$ as they capture the non-extensive or energetic particles at low probabilities and take a dominant role in the charging process. For that reason, we only consider the super-extensive case for the potential evolution. However, it is fascinating that the spacecraft potential has different patterns, such as a sudden potential-jump or a smooth transition, this happens since the space plasma parameters vary across the threshold. Huang et al. (2015) noted the reason for a potential jump from one

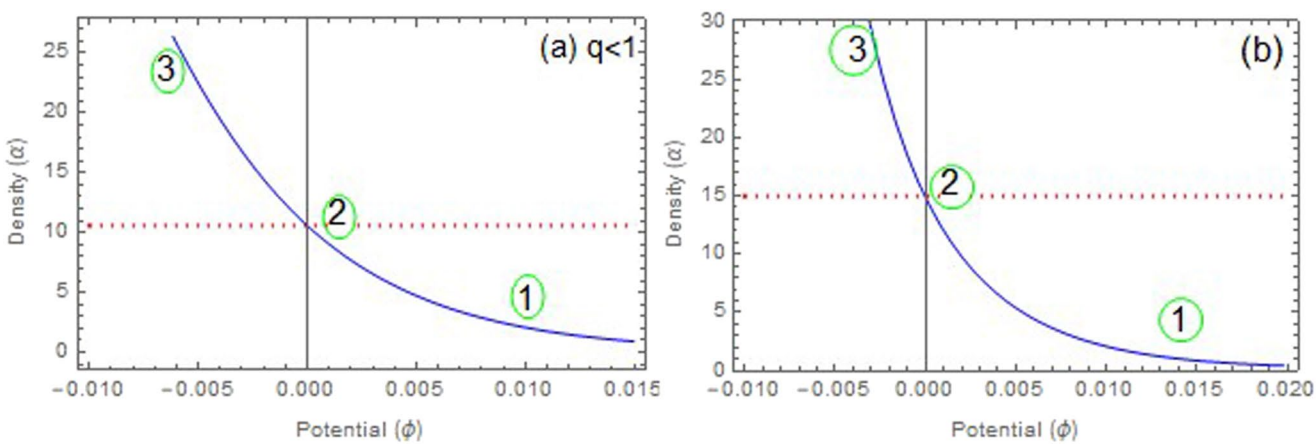

Figure 10. The variation of potential with density ratio for $T_c < T_A < T_h < T^*$ plasma parametric domain, (a) represent $q-$ non-extensive potential jump with $q = 0.8$, and (b) Maxwellian.

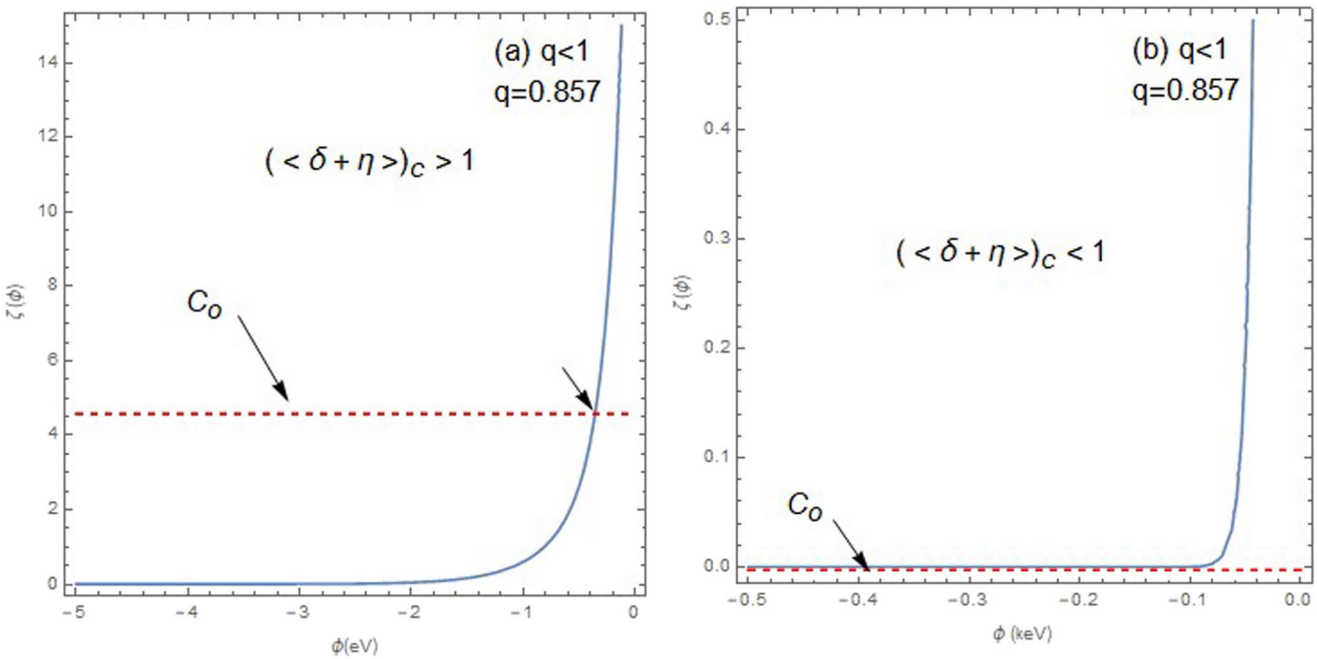

Figure 11. The comparison of function $\zeta(\phi)$ and constant C_o for $<\delta+\eta>_c > 1$ and $<\delta+\eta>_c < 1$.

potential to another potential is the transitional state that is unstable. To check the stability of negative potential at the threshold, the function $\zeta(\phi)$ and constant C_o are plotted in Figure 11a at the fixed value of temperatures and density ratio. We found that in non-extensive plasma under the limit $q < 1$, when the condition $<\delta+\eta>_c > 1$, the onset negative potential exceeds the threshold value (about 400V as represented by the arrow) as the potential curve rises earlier that they never reach to the zero potential value, thus Equation 20 is satisfied and the onset negative potential is consider to be stable. Therefore, the potential suddenly jumps from positive potential to some stable value of negative potential since the transitional states are not stable. When $<\delta+\eta>_c < 1$, Equation 21 is satisfied [see 11b], the negative potentials value is the steady state as resultant of the potential transiting smoothly from zero potential to some negative potential when the threshold condition is reached.

7. Conclusion

The threshold condition for the onset of charging in non-extensive plasma with normal incidence is theoretically studied especially in a scenario when $<\delta+\eta>_{c,h} = 1$. We have developed a model for the current balance equation on the spacecraft surface which is a function of temperature, density ratio and the non-extensivity parameter based on $q-$ non-extensive Tsallis statistics for $q < 1$ or $q > 1$. We have modified the threshold condition (for which charging can be triggered at GEO altitudes) by using the two temperatures $q-$ non-extensive distribution and summarize the results of critical and anti-critical temperatures for various surface materials presented in Table 1. However, it is found that the onset of spacecraft surface charging and charging currents can be controlled by the critical temperature of the ambient electrons and density as well, so whenever the value of the electron density ratio and the temperature of the ambient plasma is changed, the critical temperature is also changed. Furthermore, we have investigated the charging behavior with two different plasma parametric domains: $T_A < T_c < T^* < T_h$ and $T_c < T_A < T_h < T^*$. It is observed that the charging process can be initiated by a Maxwellian plasma with sufficient temperature but at high temperature, the $q-$ non-extensive distribution better illustrates the charging onset by capturing a high energy tail. We also observe that the spacecraft surface potential has different patterns when it crosses the threshold condition that is, it can suddenly jump from a positive value to some stable negative values when $\zeta(\phi) < C_o$ or it can transit smoothly from positive to the negative value at the threshold when $\zeta(\phi) > C_o$ as given in Equations 20 and 21. The impact of non-extensive particles on the distribution gives the more clear picture of spacecraft charging especially within the limit of super-extensivity $q < 1$ as they capture the high energy particles at low probabilities and a key role in initiating the charging process in

comparison to Maxwellian, while in the limit of sub-extensivity $q > 1$ the non-extensive distribution cannot lead the charging process, the reason is that the onset charging is associated with the suprathermal particles at GEO altitude but the sub-extensivity in the plasma system concerned with the low energy particles. Additionally, the charging currents due to secondary and back-scattered electrons are relatively low magnitudes in the limit $q > 1$ as compared with super-extensive case $q < 1$. Our model will provide better results for realistic measurements of critical temperature and potential on spacecraft surfaces at GEO altitude.

Appendix A

The current balance equation in two-temperature Maxwellian plasma becomes,

$$\begin{aligned}\int_0^\infty A_c \exp\left(-\frac{E}{k_B T_c}\right) E\, dE + \int_0^\infty A_h \exp\left(-\frac{E}{k_B T_h}\right) E\, dE \\ = \int_0^\infty E\left[A_c \exp\left(-\frac{E}{k_B T_c}\right) + A_h \exp\left(-\frac{E}{k_B T_h}\right)\right] \\ \times \left[c \exp\left(-\frac{E}{a}\right) - c \exp\left(-\frac{E}{b}\right) - B \exp(-EC) + A\right] dE.\end{aligned} \tag{A1}$$

Note that here $A_c\left(= n_c\left(\frac{m}{2\pi k_B T_c}\right)^{\frac{3}{2}}\right)$ and $A_h\left(= n_h\left(\frac{m}{2\pi k_B T_h}\right)^{\frac{3}{2}}\right)$ are the normalization factor of the Maxwellian distribution function. After performing integration, we get

$$\begin{aligned}A_c(k_B T_c)^2 + A_h(k_B T_h)^2 = A_c(k_B T_c)^2 \left[\begin{array}{c} c\left(\frac{a^2}{(k_B T_c + a)^2} - \frac{b^2}{(k_B T_c + b)^2}\right) \\ + A - \frac{B}{(C k_B T_c + 1)^2}\end{array}\right] \\ + A_h(k_B T_h)^2 \left[\begin{array}{c} c\left(\frac{a^2}{(k_B T_h + a)^2} - \frac{b^2}{(k_B T_h + b)^2}\right) \\ + A - \frac{B}{(C k_B T_h + 1)^2}\end{array}\right].\end{aligned} \tag{A2}$$

Now, put the values of normalization factors A_c and A_h and dividing the whole equation with factor A_h, Equation A2 simplified to

$$\begin{aligned}\alpha(k_B T_c)^{\frac{1}{2}} + (k_B T_h)^{\frac{1}{2}} = \alpha(k_B T_c)^{\frac{1}{2}} \left[\begin{array}{c} c\left(\left(1 + \frac{k_B T_c}{a}\right)^{-2} - \left(1 + \frac{k_B T_c}{b}\right)^{-2}\right) \\ + A - B(1 + C k_B T_c)^{-2}\end{array}\right] \\ + (k_B T_h)^{\frac{1}{2}} \left[\begin{array}{c} c\left(\left(1 + \frac{k_B T_h}{a}\right)^{-2} - \left(1 + \frac{k_B T_h}{b}\right)^{-2}\right) \\ + A - B(1 + C k_B T_h)^{-2}\end{array}\right].\end{aligned} \tag{A3}$$

$$\begin{aligned}\alpha(k_B T_c)^{\frac{1}{2}} + (k_B T_h)^{\frac{1}{2}} = \alpha(k_B T_c)^{\frac{1}{2}} \left[\zeta_\delta(k_B T_c) + \zeta_\eta(k_B T_c)\right] \\ + (k_B T_h)^{\frac{1}{2}} \left[\zeta_\delta(k_B T_h) + \zeta_\eta(k_B T_h)\right].\end{aligned} \tag{A4}$$

where $\alpha\left(= \frac{n_c}{n_h}\right)$ is ratio of two densities and ζ_δ, ζ_η are the averaged yield of secondary and backscattered electrons emission respectively, that may be described as

$$\zeta_\delta(k_B T_{c,h}) = c\left(\left(1 + \frac{k_B T_{c,h}}{a}\right)^{-2} - \left(1 + \frac{k_B T_{c,h}}{b}\right)^{-2}\right)$$

$$\zeta_\eta(k_B T_{c,h}) = A - B(1 + C k_B T_{c,h})^{-2}$$

Equation A4 can also be written as

$$\frac{\alpha(k_B T_c)^{\frac{1}{2}} < \delta + \eta >_c + (k_B T_h)^{\frac{1}{2}} < \delta + \eta >_h}{\alpha(k_B T_c)^{\frac{1}{2}} + (k_B T_h)^{\frac{1}{2}}} = 1 \quad \text{(A5)}$$

$<\delta + \eta>_{c,h}$denoting the average of secondary and back-scattered electrons yield in terms of two plasma components that is, hot and cold

$$< \delta + \eta >_c = \zeta_\delta(k_B T_c) + \zeta_\eta(k_B T_c)$$
$$< \delta + \eta >_h = \zeta_\delta(k_B T_h) + \zeta_\eta(k_B T_h)$$

Data Availability Statement

Data were not used, nor created for this research.

Acknowledgments
One of the author NR would like to thank the Centre for Mathematical Plasma-Astrophysics for providing the partial funding and facilitating the research and publication process. The author would also like to thank HEC for providing financial assistance through Refs: 3-1/PDFP/HEC/2021/420/01 and 20-15574/NRPU/R&D/HEC/2021-2020. Sp acknowledges support from the projects C14/19/089 (C1 project Internal Funds KU Leuven), G.0B58.23N and G.0025.23N (FWO-Vlaanderen), SIDC Data Exploitation (0ESA Prodex-12), and Belspo project B2/191/P1/SWiM.

References

Ali, S., Rubab, N., Nawaz, K., & Sarwar, S. (2020). A comparative study of spacecraft charging onset at geosynchronous altitudes: A nonextensive particle approach. *Journal of Geophysical Research: Space Physics*, *125*(9), e2020JA028107. https://doi.org/10.1029/2020ja028107

Boon, J. P., & Tsallis, C. (2005). Special issue overview nonextensive statistical mechanics: New trends, new perspectives. *Europhysics News*, *36*(6), 185–186. https://doi.org/10.1051/epn:2005601

Chaudhry, M., & Zubair, S. M. (1992). Remarks on the Whittaker functions. *Applied Mathematics Letters*, *5*(5), 25–29. https://doi.org/10.1016/0893-9659(92)90057-G

Craven, P., Olsen, R., Fennell, J., Croley, D., & Aggson, T. (1987). Potential modulation on the SCATHA spacecraft. *Journal of Spacecraft and Rockets*, *24*(2), 150–157. https://doi.org/10.2514/3.25888

DeForest, S. E. (1972). Spacecraft charging at synchronous orbit. *Journal of Geophysical Research*, *77*(4), 651–659. https://doi.org/10.1029/ja077i004p00651

DeForest, S. E. (1973). Electrostatic potentials developed by ATS-5. In *Photon and particle interactions with surfaces in space: Proceedings of the 6th ESLAB symposium, held at Noordwijk, The Netherlands* (pp. 263–267).

Dereziński, J., & Richard, S. (2018). On radial Schrödinger operators with a Coulomb potential. *Annales Henry Poincare*, *19*(9), 2869–2917. https://doi.org/10.1007/s00023-018-0701-7

Engelhart, D. P., Plis, E. A., Ferguson, D., Johnston, W. R., Cooper, R., & Hoffmann, R. C. (2019). Space plasma interactions with spacecraft materials. *Plasma Science and Technology-Basic Fundamentals and Modern Applications*, 225–245.

Ferguson, D. C., Hilmer, R. V., & Davis, V. A. (2015). Best geosynchronous earth orbit daytime spacecraft charging index. *Journal of Spacecraft and Rockets*, *52*(2), 526–543. https://doi.org/10.2514/1.a32959

Garrett, H. B. (1981). The charging of spacecraft surfaces. *Reviews of Geophysics*, *19*(4), 577–616. https://doi.org/10.1029/rg019i004p00577

Harris, J. T. (2003). Spacecraft charging at geosynchronous altitudes: Current balance and critical temperature in a non-Maxwellian plasma.

Huang, J., Liu, G., & Jiang, L. (2015). Threshold for spacecraft charging in double-Maxwellian plasma. *Journal of Geophysical Research: Space Physics*, *120*(8), 6301–6308. https://doi.org/10.1002/2015ja021173

Huang, J., Liu, G., Jiang, L., & Yang, Y. (2017). Theory for geosynchronous spacecraft charging index. *Space Weather*, *15*(9), 1203–1211. https://doi.org/10.1002/2017sw001670

Lai, S., & Tautz, M. (2008). On the anticritical temperature for spacecraft charging. *Journal of Geophysical Research*, *113*(A11), A11211. https://doi.org/10.1029/2008JA013161

Lai, S. T. (1991). Spacecraft charging thresholds in single and double Maxwellian space environments. *IEEE Transactions on Nuclear Science*, *38*(6), 1629–1634. https://doi.org/10.1109/23.124155

Lai, S. T. (2010). Importance of surface conditions for spacecraft charging. *Journal of Spacecraft and Rockets*, *47*(4), 634–638. https://doi.org/10.2514/1.48824

Lai, S. T. (2012). *Fundamentals of spacecraft charging: Spacecraft interactions with space plasmas*. Princeton University Press.

Lai, S. T., & Della-Rose, D. J. (2001). Spacecraft charging at geosynchronous altitudes: New evidence of existence of critical temperature. *Journal of Spacecraft and Rockets*, *38*(6), 922–928. https://doi.org/10.2514/2.3764

Lai, S. T., & Tautz, M. (2006). High-level spacecraft charging in eclipse at geosynchronous altitudes: A statistical study. *Journal of Geophysical Research*, *111*(A9), A09201. https://doi.org/10.1029/2004ja010733

Livadiotis, G., & McComas, D. (2013). Understanding kappa distributions: A toolbox for space science and astrophysics. *Space Science Reviews*, *175*(1–4), 183–214. https://doi.org/10.1007/s11214-013-9982-9

Morse, P. M., & Feshbach, H. (1953). *Methods of theoretical physics* (Vol. i, p. 997). McGraw-Hill.

Mullen, E., Gussenhoven, M., Hardy, D., Aggson, T., Ledley, B., & Whipple, E. (1986). Scatha survey of high-level spacecraft charging in sunlight. *Journal of Geophysical Research*, *91*(A2), 1474–1490. https://doi.org/10.1029/ja091ia02p01474

Olsen, R. C. (1981). Modification of spacecraft potentials by thermal electron emission on ATS-5. *Journal of Spacecraft and Rockets*, *18*(6), 527–532. https://doi.org/10.2514/3.28068

Pervaiz, F., Ali, S., Ali, M., & Lai, S. T. (2023). Spacecraft charging due to energetic electrons and ions at geosynchronous altitudes. *Journal of Geophysical Research: Space Physics*, *128*(1), e2022JA030642. https://doi.org/10.1029/2022ja030642

Prokopenko, S., & Laframboise, J. (1980). High-voltage differential charging of geostationary spacecraft. *Journal of Geophysical Research*, *85*(A8), 4125–4131. https://doi.org/10.1029/ja085ia08p04125

Rubin, A., Garrett, H., Wendel, A., & Laboratory, U. A. F. G. (1980). *Spacecraft charging on ATS-5. Air force geophysics laboratory*. Air Force Systems Command, United States Air Force. Retrieved from https://books.google.com.pk/books?id=KNJA3aVGZSkC

Saberian, E., & Esfandyari-Kalejahi, A. (2014). Kinetic theory of acoustic-like modes in nonextensive pair plasmas. *Astrophysics and Space Science*, *349*(2), 799–811. https://doi.org/10.1007/s10509-013-1678-9

Safa, N. N., Ghomi, H., & Niknam, A. (2015). Plasma immersion ion implantation characteristics with q-nonextensive electron velocity distribution. *Journal of Plasma Physics*, *81*(3), 905810303. https://doi.org/10.1017/s0022377814000981

Sanders, N., & Inouye, G. (1979). Secondary emission effects on spacecraft charging: Energy distribution considerations. In *Spacecraft charging technology-1978* (Vol. 2071, p. 747).

Tsallis, C. (1988). Possible generalization of Boltzmann-Gibbs statistics. *Journal of Statistical Physics*, *52*(1–2), 479–487. https://doi.org/10.1007/BF01016429

Tsallis, C. (1994). Nonextensive physics: A possible connection between generalized statistical mechanics and quantum groups. *Physics Letters A*, *195*(5–6), 329–334. https://doi.org/10.1016/0375-9601(94)90037-x

Tsallis, C., Gell-Mann, M., & Sato, Y. (2005). Extensivity and entropy production. *Europhysics News*, *36*(6), 186–189. https://doi.org/10.1051/epn:2005602

Vasyliunas, V. M. (1968). Low-energy electrons on the day side of the magnetosphere. *Journal of Geophysical Research*, *73*(23), 7519–7523. https://doi.org/10.1029/ja073i023p07519

Whipple, E. C. (1981). Potentials of surfaces in space rep. *Progress of Physics*, *44*, 1198.

Yoon, P. H. (2019). Thermodynamic, non-extensive, or turbulent quasi-EQUILIBRIUM for the space plasma environment. *Entropy*, *21*(9), 820. https://doi.org/10.3390/e21090820